6th IEEE RAS/EMBS International Conference on
Biomedical Robotics and Biomechatronics (BioRob)
June 26-29, 2016. UTown, Singapore

Surface Tilt Perception with a Biomimetic Tactile Sensor

Zhe Su, *Student Member*, Stefan Schaal, *Senior Member*, and Gerald E. Loeb, *Senior Member*

***Abstract*— Humans are known to be good at manipulating tools. To cope with disturbances and uncertainties from the external environment during such tasks, they must be able to perceive small changes in orientation or tilt of the tool using mechanoreceptors in the glabrous skin of the fingertips. We hypothesize that the most sensitive part of human fingers, a flat surface on the distal phalanx (called apical tuft) would be preferred for perceiving very fine tilts. In this paper, we used an experimental apparatus to quantify discrimination threshold of a biomimetic tactile sensor (BioTac®) that incorporates a similar, sensorized flat surface. We found the thresholds to be as small as 0.11º for tilts in the roll direction and 0.19º for tilts in the pitch direction. The flat surface was superior in detecting tilts when compared to other, curved locations on the BioTac.**

I. Introduction

A service robot deployed in human environments must be able to perform dexterous manipulation tasks with hand-held tools, such as sewing, scraping, and wiping. Tool-use can reduce wear on end-effectors and enable increased dexterity by enabling the robot to manipulate objects or work in spaces that are too small for its unaided grippers. Compliant grippers such as found on "soft robots" are similar to human fingertips in reducing the demands for precision and speed in response to contact forces but they require a means to sense the precise current orientation of the tool in order to plan the next step in the task. Humans gripping a pencil shaft 5 cm from the tip must be aware of the position of the tip with about 2 mm accuracy to produce legible handwriting, which corresponds to sensing a 2º tilt of the pencil shaft with respect to the highly compliant skin and pulp of the fingertips.

To achieve a human-level of performance in tool-use, a robot is likely to require tactile sensors. A variety of tactile sensors have been designed [1] but their use to solve various problems in robotic grasping and manipulation is still in the early stages. Previous research into robotic tool-use with tactile sensing has mainly focused on using pixel-type tactile arrays to do adaptive control for pose uncertainties between tools and environment [2], [3].

This research was supported by the Max Planck Institute for Intelligent Systems. BioTac sensors were provided by SynTouch LLC. Gerald Loeb is an equity partner in SynTouch LLC, manufacturer of the BioTac sensors used in this research.

Zhe Su is with the Computational Learning and Motor Control Lab, University of Southern California, Los Angeles, CA 90089, USA. E-mail: zhesu@usc.edu.

Stefan Schaal is with the Computational Learning and Motor Control Lab, University of Southern California, Los Angeles, CA 90089, USA, and the Autonomous Motion Department, Max-Planck Institute for Intelligent Systems, Tubingen, Germany. E-mail: sschaal@usc.edu.

Gerald E. Loeb is with the Medical Device Development Facility, University of Southern California, CA 90089, USA and SynTouch LLC, Los Angeles, CA, USA. E-mail: gloeb@usc.edu.

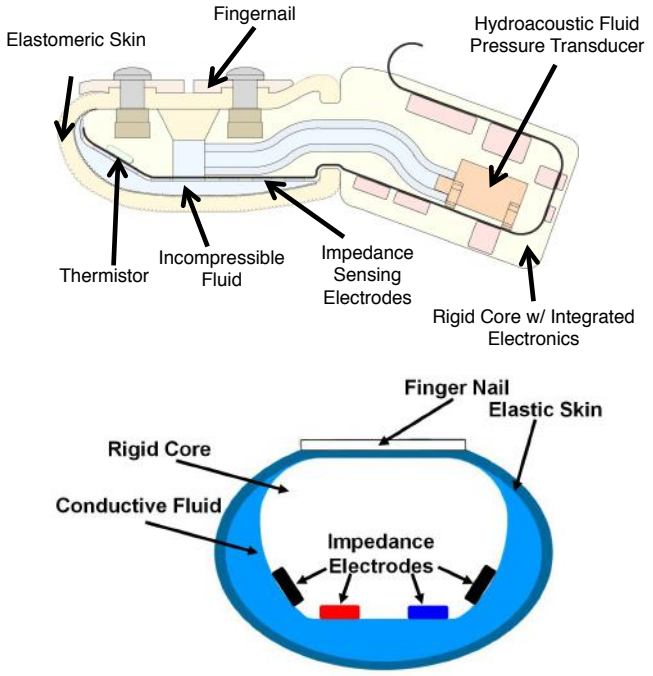

Figure 1. Cross-sectional schematics of the BioTac sensor.

Recently, a biomimetic tactile sensor (BioTac®), designed to provide all sensing modalities and mechanical properties of human fingertips, has been developed. Each BioTac (see Fig. 1) consists of a rigid core housing an array of 19 electrodes surrounded by an elastic skin. The skin is inflated with an incompressible and conductive liquid. When the skin is in contact with an object, the liquid is displaced, resulting in distributed conductance changes in the electrode array on the surface of the rigid core. The conductance of each electrode tends to be dominated by the thickness of the liquid between the electrode and the immediately overlying skin. The skin has a pattern of asperities on its inner surface that gradually compress with increasing normal force, greatly increasing the dynamic force range [4]. The distributed conductance changes can be used to detect the point of contact, the magnitude and orientation of the force vector, compliance [5], and object spatial properties [6], [7]. The conductance of each electrode is measured as a voltage induced by a brief, current regulated pulse and digitized (100 samples/s at 12 bits resolution) in the BioTac for serial data transmission. As described in more detail below, four of these electrodes are located on a small flat surface of the rigid core that corresponds to a similar feature of the human distal phalanges (Fig. 2b).

In this work, we use the BioTac to detect small tilt angles of a flat surface, which is crucial in tool-use. The key contributions of this work are: a) a comprehensive comparison between human apical tuft and BioTac, b) an

apparatus to quantify the discrimination thresholds of tilts, c) a demonstration that a biomimetic tactile sensor can detect static tilt in roll and pitch that is suitable for tool use and may provide insights into human perception.

II. Comparison of Human Apical Tuft and a Biomimetic Tactile Sensor

A. Anatomy

In the human hand, the distal end of each distal phalanx possesses a flat expansion called an apical tuft (also known as an ungual ruberosity or process), which serves to support the fleshy pad or pulp on the volar side of the fingertips and the nails on the dorsal side [8]. Two lateral ungual spines project proximally from the apical tuft, see Fig. 2a. The pairs of ungual spines on the human thumb are asymmetric (the ulnar side being more prominent) to ensure that the thumb pulp is always facing the pulps of the other digits, an osteological configuration which maximizes contact surface with held objects [9]. Humans tend to use a "precision grip" to hold small tools, in which the apical tufts of the opposing fingers are parallel to each other and to the surfaces of the tool [10].

The shape of the molded epoxy core of the BioTac was based on careful measurements of a human distal phalanx bone. As shown in Fig. 2b, the rigid core of the BioTac consists of a spherical region and a cylindrical region, which can be approximated as one-quarter of a sphere, and one-half of a cylinder, respectively. On the spherical region, a flat surface at a 30-degree angle was developed to mimic the human apical tuft.

B. Evolutionary Development

Susman [11] and Shrewsbury and Johnson [12] have shown that humans have proportionately broader and more robust apical tufts on the distal phalanges than other extant primates. The widened apical tufts support broad, palmar, fibrofatty pads whose large surfaces distribute pressure during forceful grasping and whose deformation accommodates the pads to uneven surfaces as well as fine-tuning in the positioning of objects [11], [13], [14]. From an evolutionary point of view, the widened tufts and the large frictional surface would have been essential for securing and controlling cradle precision pinch of large preforms and three-jaw "baseball" grip of hammerstones in habitual tool making and tool using [15], [16]. Compared to chimpanzees and hamadryas baboons, human pad-to-pad precision grips are distinguished by the greater force with which objects may be secured by the thumb and fingers of one hand (precision pinching) and the ability to adjust the orientation of gripped objects through movements at joints distal to the wrist (precision handling) [17].

C. Mechanical Properties

Measurements of the contact force and fingertip displacement as individuals tap on a flat, rigid surface [18] or grasp an object between the thumb and index finger [19] indicate that it is a nonlinear spring in which most of the displacement of the fingertip pulp occurs at forces of less than 1N (red dots in Fig. 3). At higher forces, the pulp stiffens rapidly from around 3.5N/mm at 1N to over 20N/mm at 4 N, which mechanically protects the distal phalanx from impact [18].

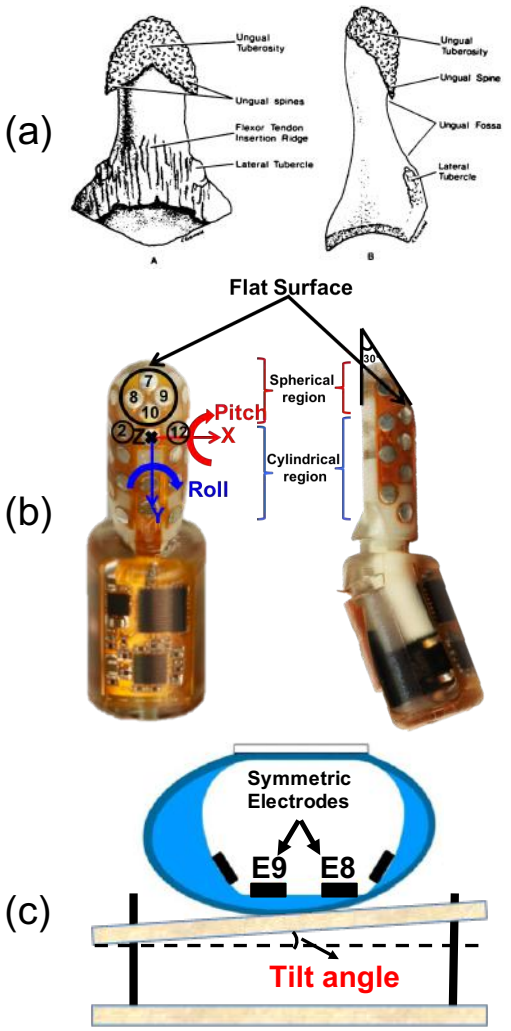

Figure 2. (a). A volar view of the distal phalanx (A), and a lateral view of the distal phalanx (B). Source: [8]; (b). Side and ventral views of the rigid core of the BioTac; (c). Cross-sectional view of the BioTac pressed vertically against the test apparatus, whose tilt could be precisely adjusted and accurately measured.

The core of the BioTac is surrounded by an elastomeric skin (Dow Corning Silastic S, Shore A 26) and the space between the skin and the core is inflated with an incompressible fluid (water with NaBr and polyethylene glycol) to give it compliance similar to the human fingertip. The displacement of the fingertip of the BioTac was measured by a linear motor that pressed a flat aluminum plate against the BioTac, and the force between the BioTac and the flat plate was measured by a six-axis force plate (AMTI HE6x6-16) supporting the BioTac (blue circles in Fig. 3). The relationship between the displacement and force was estimated with a 8th-order polynomial function, and the stiffness of the BioTac at 1 and 4N were the first derivative of the force-displacement polynomial function at those specific forces. The stiffness of the BioTac at 1 and 4N are 3.38N/mm and 14.53N/mm, respectively. The texturing of the inner surface of the skin provides sensitivity for transduction of relatively small compression changes that occur in the high force – high stiffness range of the BioTac [4].

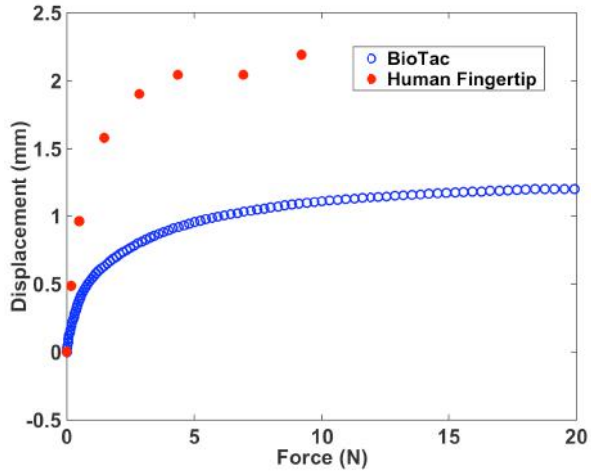

Figure 3. The force-BioTac displacement data (open blue circles) during contact with a flat rigid surface (inflation volume 0.15ml, inflation pressure 11721.1 Pa according to factory specifications); the force-fingertip displacement data (red dots) as one human subject taps his or her fingertip on a flat, rigid surface. Redrawn from [25].

D. Sensory Transduction

Primate glabrous skin over the area of the apical tuft contains a higher density of Merkel cells, which are highly sensitive to local skin stress/strain [20], [21]. These cells are innervated by slowly adapting, low-threshold afferents (SA-I afferent fiber) with small receptive fields [22]. SA-I afferents are particularly sensitive to spatial features, such as points, edges, curvature and orientation [23], and their population responses have been shown to encode the representation of these spatial features independent of contact forces [24].

Similarly to the human apical tuft, the flat surface on the core of the BioTac is equipped with a cluster of four identical electrodes, including electrodes 8 and 9 symmetrically distributed along the Y-axis, or the roll direction in the finger coordinate frame, and electrodes 7 and 10 symmetrically distributed along the X-axis, or the pitch direction in the finger coordinate frame (Fig. 2b). If the flat surface is oriented parallel to a contact surface while pressing the skin against it, the four electrodes should generate the same voltage values as normal force increases symmetrically on all four electrodes [5]. Even slight rotations or tilts of the sensor from parallel alignment with a contacting surface will produce large asymmetries in skin deformation, which could be sensed by the voltage differences between each pair of electrodes. For example, the voltage differences between electrodes 8 and 9 can be used to detect the tilt angle along the roll direction in the finger coordinate frame, as shown in Fig. 2c. Therefore, the voltage asymmetries can be used to achieve very fine perception and control of the orientation of the fingertip with respect to a contacting surface.

E. Tilt Perception

Tilt perception has been studied directly in a couple of human psychophysical studies, although not in configurations related to precision grip. For example, tilt perception has been measured in subjects attempting to discriminate angular differences between a pair of planar surfaces [26], [27]. The subjects could freely trace these two-dimensional angles with the index fingers of their outstretched arms. The discrimination threshold for 75% correct performance was 5.2°. Tilt perception has also been studied indirectly as perception of local curvature in various psychophysical and neurophysiological studies on primates. For example, Wijntjes et al. showed that local surface orientation dominates haptic curvature perception using both virtual shapes created on a haptic device and real shapes [28].

In robotics, De Maria et al. have proposed using a tactile sensor array to estimate the relative orientation difference between robot finger frame and object frame so that the measured contact forces on the finger frame can be corrected to estimate coefficient of friction in the object frame [29]. They have shown that their method could estimate the orientation of a flat surface from 2° to 25° with maximal error less than 2° [30].

III. Methods

A. Discrimination Threshold of Tilt

In psychophysics, discrimination threshold is usually used to quantify perceptual resolution. It measures the smallest difference between two stimuli that the subject is able to detect some proportion of the time (75% correct detection is often used). The discrimination threshold depends on various types of noise in the system, including sensor noise, motor noise in the exploratory movement, and nonstationarity of the external environment.

In a robotic system, the sensors will have electronic and digitization noise and the grip force may be subject to motor noise. For a robotic system to discriminate differences in tilt angles with a biomimetic sensor, two assumptions have to be made: 1) every sample of the voltage value on the electrodes can be used to estimate tilt angles; 2) the perception of a tilt angle can be modeled as a normal distribution centered at the voltage asymmetries on each pair of symmetric electrodes. The standard deviation will include electronic noise from the sensor and uncertainties of grip force.

As shown in Fig. 4, we define discrimination threshold of tilt as the smallest differences between two tilt angles ($angle_1$, $angle_2$) at which two corresponding normal distributions (in blue and red), which are centered at two corresponding voltage asymmetries (Diff(E8, E9)) on a pair of symmetric

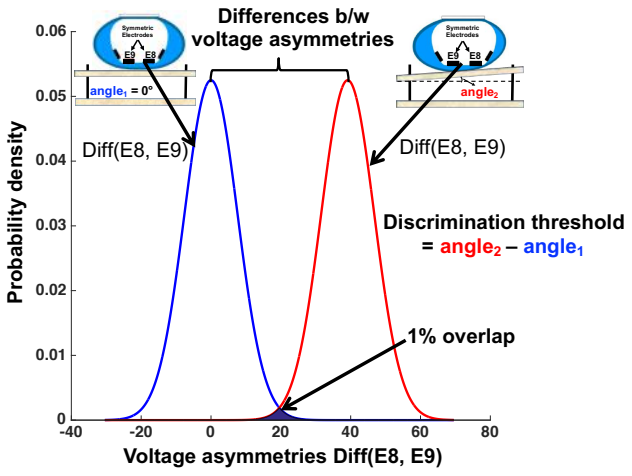

Figure 4. An illustration of definition of discrimination threshold of tilt on a biomimetic tactile sensor.

electrode 8 (E8) and electrode 9 (E9), have less than 1 percent overlap even with their respective electronic noise on the conductance-sensing electrode, and asymmetric voltage caused by uncertainties of total normal contact (grip) force. The electronic noise and the uncertainties of total normal contact force contribute to the standard deviation of these two normal distributions.

B. Apparatus

The BioTac was mounted on a rigid arm that could be oriented at various angles to horizontal and lowered vertically with a micromanipulator onto the test surface. The test surface was mounted on a force plate (AMTI HE6x6-16) via threaded vertical rods that could be adjusted with pairs of wingnuts to create static tilts of ±10º in pitch and/or roll with respect to the BioTac (indicated in Fig. 5 and schematically in Fig. 2c). Two digital protractors with 0.1-degree resolution (Wixey WR300 Digital Angle Gauge) were used to measure the tilt angles during the experiment (shown in Fig. 5). Data were collected from the BioTac sensor and the force plate in LabVIEW at 100 samples/s using a NI USBSPI/I2C-8451 data acquisition device. For the experiments reported here, two orientation angles were used: 30º corresponding to the BioTac flat surface oriented horizontally and 10º corresponding to the BioTac tilted up in pitch so that its cylindrically curved portion would make first contact with a horizontal surface.

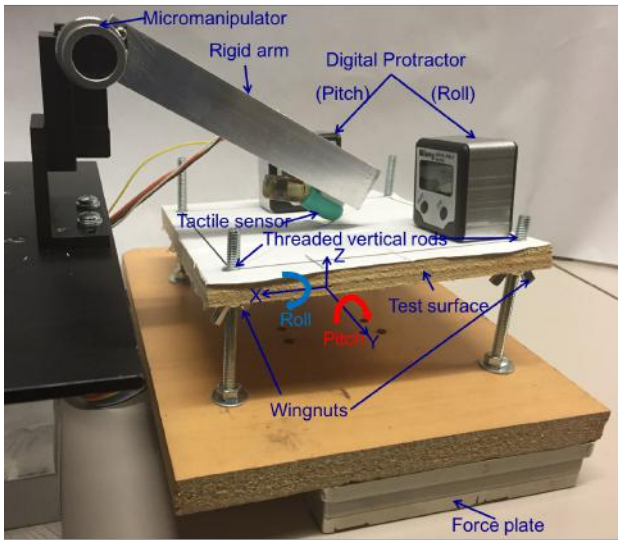

Figure 5. Experimental setup.

C. Data collection Procedure

In order to align the BioTac with the tilt stage, the flat surface on the spherical region of the BioTac was lowered with the micromanipulator to press against the tilt stage with 6N normal contact force F_z (downward = positive) on the force plate. Then, the orientations along the roll and pitch directions of the tilt stage were adjusted to achieve matched voltage readings for electrodes 7 and 10 (X-axis for pitch) and electrodes 8 and 9 (Y-axis for roll). Both digital protractors were then set to zero.

To measure the discrimination threshold to tilt, we fixed one orientation of the tilt stage to 0º and systematically changed the other direction of rotation on the tilt plate over ±7º with 0.5º per step. At each combination of tilt angles in the pitch and the roll directions, we manually moved the micromanipulator to press the BioTac against the tilt stage with the desired normal (Z-axis) force, and we repeated this 20 times.

To measure the effect of pitch angle on the discrimination threshold to tilt in the roll direction, we pressed the BioTac 20 times on the tilt stage with the roll direction varied over ±7º with 0.5º per step, and repeated this for a wide range of angles in the pitch direction on the tilt stage from -30º to +7º with 1º per step. We also studied the effect of roll angle on the discrimination threshold to tilt in the pitch direction by pressing the BioTac 20 times on the tilt stage with the pitch direction varied over ±7º with 0.5º per step, and repeated this at angles in the roll direction on the tilt stage from 0º to +7º with 0.5º per step. The range of angles in the roll direction is limited by the experimental setup, shown in Fig. 5. Because the BioTac is symmetric along its roll direction, the discrimination thresholds for the negative roll direction (-7 ~ 0º) should be similar to the discrimination thresholds for the positive roll direction (0 ~ +7º) measured in our experiments.

Finally, we used the full dataset to study the discrimination threshold to tilt in the roll direction using different structural locations of the BioTac, such as comparing the discrimination threshold to roll with the symmetric pair of electrodes 8 and 9 on the flat surface to the discrimination threshold to roll with the symmetric pair of electrodes 2 and 12 on the half cylindrical part of the BioTac.

IV. Results

A. Discrimination Thresholds of Tilts with the Flat Surface on the BioTac Assuming only Electrical Noise

Fig. 6 shows typical examples of the discrimination thresholds of tilts with the flat surface of the BioTac with only electronic noise. The flat surface of the BioTac was pressed against the tilt stage with 0º in pitch direction, and -7

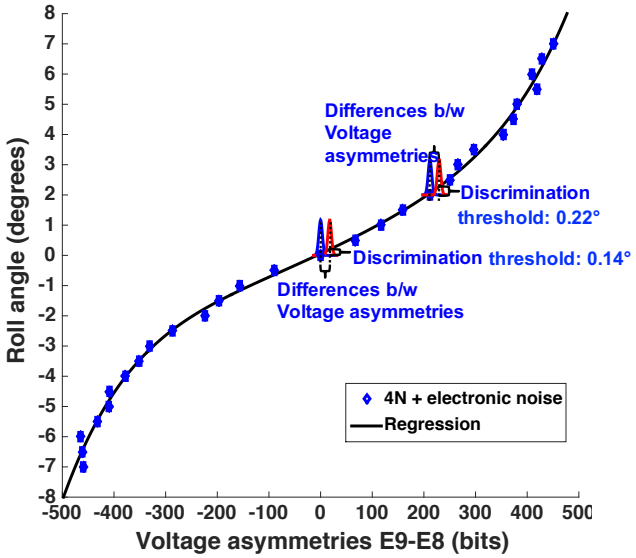

Figure 6. Typical examples of discrimination thresholds of tilt angles in the roll direction with only electronic noise on the impedance-sensing electrodes (normal contact force at 4N).

to +7° with 0.5° per step in roll direction, applying 4N normal contact force. Each data point on the figure indicates the mean voltage asymmetries on paired electrodes 8 and 9 (in units corresponding to 12-bit digitization of the 3.3V dynamic range of the input signals); the error bars indicate the positive and negative standard deviations of electrical noise on this pair of electrodes. These mean voltage asymmetries were fitted to a 5th order polynomial regression, the black curve in Fig. 6.

To find the discrimination threshold at 0° tilt in the roll direction, the tilt perception of the sensor is modeled by a normal distribution centered at the mean voltage asymmetries corresponding to 0° in the roll direction with standard deviation due to the electronic noise, the blue normal distribution centered at 0° in Fig. 6. Another normal distribution with the same standard deviation as the standard deviation at 0°, shown in red neighbored to the blue normal distribution centered at 0°, is used to search for the mean voltage asymmetries to satisfy 1 percent overlap between these two normal distributions. Then we can calculate the differences between two tilt angles corresponding to these two mean voltage asymmetries with the 5th order polynomial regression equation. Thus, when the flat surface of the BioTac is parallel with a tilted surface in the roll direction, the discrimination threshold to tilt angle in roll is 0.14°. When the flat surface of the BioTac is already 2° tilted in the roll direction, the discrimination threshold to tilt angle in roll is almost doubled to 0.22°.

At the same level of normal contact force, the discrimination thresholds of tilts along the roll direction increased with the increases in roll angles (see the discrimination thresholds at 4N and 5N in Fig. 7). The discrimination thresholds of the positive and the negative angles are almost symmetric along the 0-degree tilt angle in the roll direction, and it is consistent with the symmetrical structure of the BioTac along the Y-axis (Fig. 2b). The discrimination thresholds of tilts along the roll direction also decreased significantly with increases in normal contact forces. The slight asymmetries in the discrimination thresholds along the 0-degree tilt in the roll direction could be caused by two sources: 1) The flat surface of the BioTac and the flat surface were not perfectly parallel when we set the digital protractors to zero. 2) The exact shapes of the BioTac electrodes and their interactions with the overlying skin may not be perfectly symmetrical.

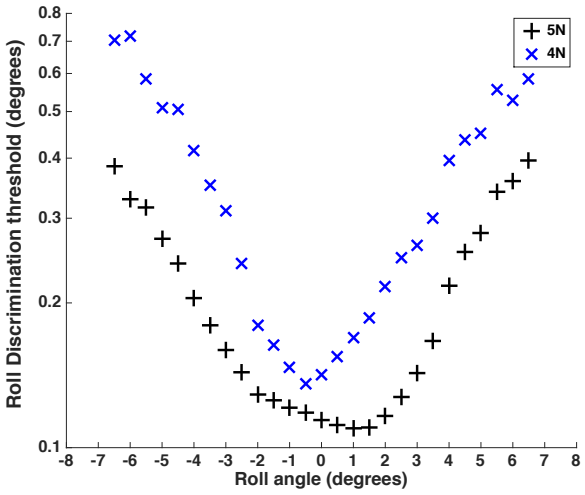

Figure 7. Discrimination thresholds (log scale) of tilts along roll direction under only electronic noise at two levels of contact normal force.

As shown in Fig. 8, the discrimination thresholds for tilts along both the positive and negative pitch direction also increased with the increases of angle along the pitch direction but the relationship was markedly asymmetrical. This would be consistent with the asymmetric structure of the BioTac along the X-axis.

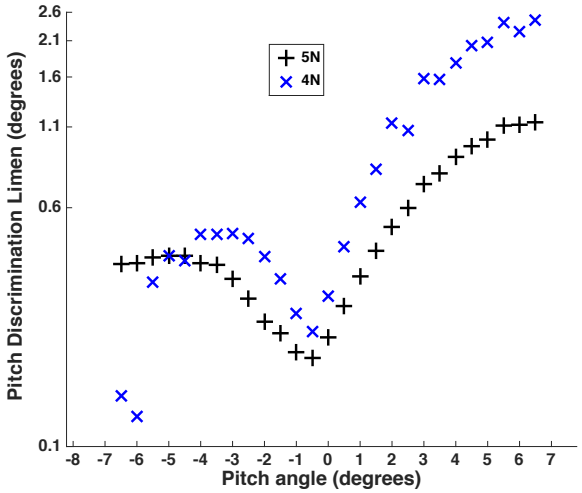

Figure 8. Discrimination thresholds (log scale) of tilts along pitch direction under only electronic noise at two levels of contact normal force.

B. Discrimination Threshold of Tilt with the Flat Surface on the BioTac Under Both Electronic Noises and Force Uncertainties

Under typical use conditions on a motor-actuated robot, the normal force being applied to an object by the contacting surface(s) of the robot would be subject to noise in the sensors and control algorithms used to control the contact force. Fig. 9 shows typical examples of the discrimination

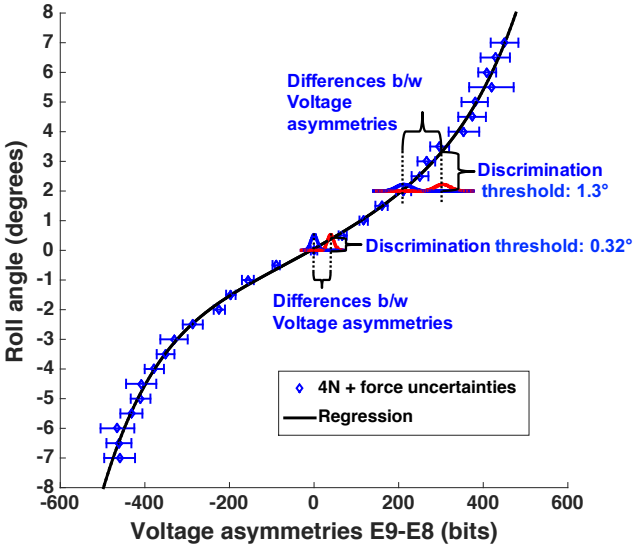

Figure 9. Typical examples of discrimination thresholds of tilt angles in the roll direction with both electronic noises on the impedance-sensing electrodes and uncertainties on the normal contact force (normal contact force in the range of 3.95N to 4.05N).

thresholds of tilts with the flat surface of the BioTac in which normal force fluctuates unpredictably according to a normal distribution with a standard deviation of 0.05N (1.25% of 4N). Because the individual electrodes of the BioTac are sampled serially, uncertainties in force at the time of sampling result in much larger uncertainties in the symmetry of those measurements. The mean voltage asymmetries on pair electrodes 8 and 9 are the same as Fig. 6, but the error bars indicate both the positive and negative standard deviation assuming both electronic and force noise. When the flat surface of the BioTac is at 0º (or parallel) in roll to the tilted surface, the discrimination threshold to tilt angle in roll is 0.32º. When the flat surface of the BioTac is already 2º tilted off in the roll direction, the discrimination threshold to tilt angle in roll almost quadrupled to 1.3º.

At the same level of normal contact force, the discrimination thresholds for tilts along the roll direction increased with increases in angle along both the positive and the negative direction along the roll direction (compare Fig. 10 to Fig. 7, which has a much finer scale on the ordinate). The discrimination thresholds of the positive and the negative angles are almost symmetric along the 0-degree tilt angle along the roll direction, and it is also consistent with the symmetrical structure of the BioTac along the Y-axis (Fig. 2a). The discrimination threshold of tilt along the roll direction also decreased with increases in normal contact forces.

The discrimination thresholds of tilts along both the positive and negative pitch direction also increased with the increases of angle along the pitch direction (compare Fig. 11 to Fig. 8, which has a much finer scale on the ordinate). However, the discrimination thresholds of tilts along the positive pitch direction were much larger than the discrimination thresholds of tilts along the negative pitch direction. This was also consistent with the asymmetric structure of the BioTac along the X-axis.

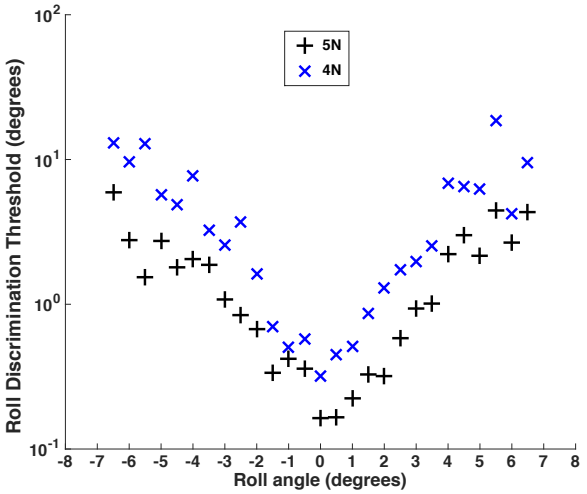

Figure 10. Discrimination thresholds (log scale) of tilts along roll direction under both electronic noises and force uncertainties (two levels of contact normal force).

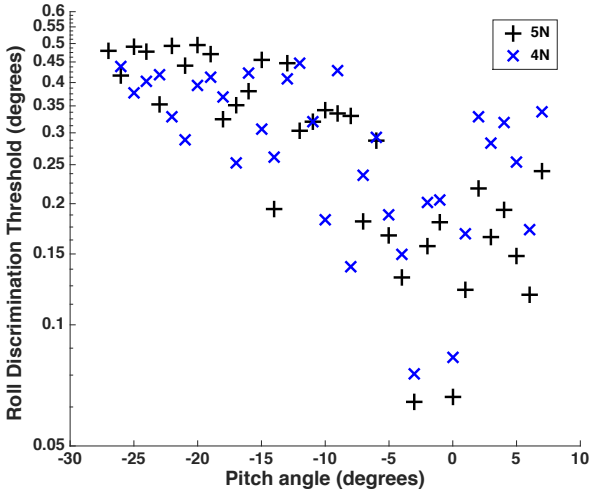

Figure 12. Effect of different pitch angles on the discrimination thresholds (log scale) for 0-degree tilt along the roll direction under only electronic noises.

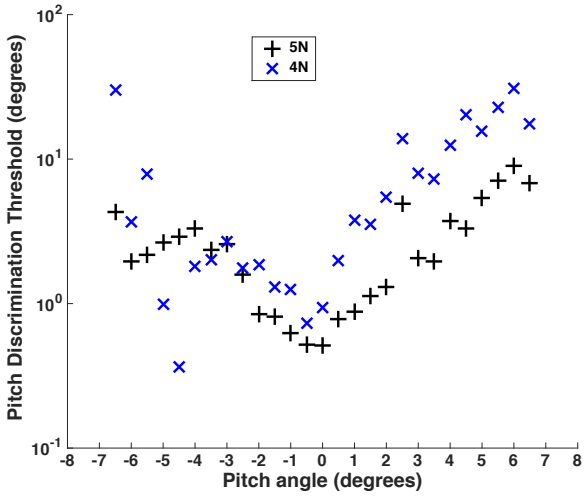

Figure 11. Discrimination threshold (log scale) of tilts along pitch direction under both electronic noises and force uncertainties (three levels of contact normal force).

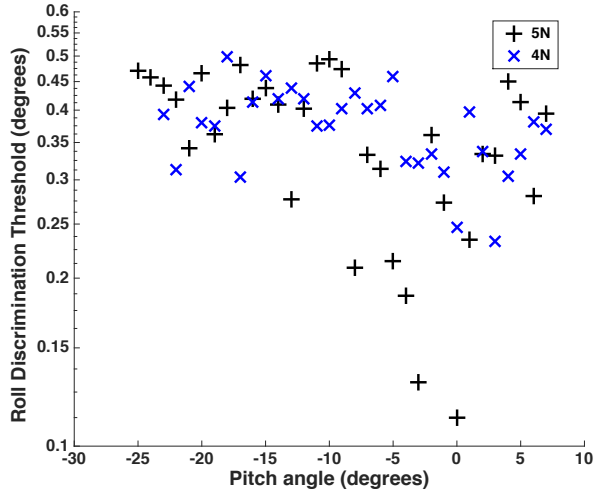

Figure 13. Effect of different pitch angles on the discrimination thresholds (log scale) for 0-degree tilt along the roll direction under both electronic noises and uncertainties in normal contact force.

C. *Effect of Tilt Angles in One Axis on the Discrimination Thresholds for Tilts in Another Axis*

When considering only electronic noise, the discrimination threshold for 0-degree tilt in the roll direction increased with increases of tilt in both the positive and the negative pitch direction (0º to +7º and 0º to -27º); see Fig. 12. The differences between voltage asymmetries on pair electrodes 8 and 9 could not be used to detect tilts in roll once the pitch angle was more negative than -27º. In this position, the unsensorized tip of the BioTac bears virtually all of the applied force and the voltage asymmetries between electrodes 8 and 9 were always smaller than background noise.

When considering both electronic noise and uncertainties in normal contact force, the discrimination threshold for 0-degree tilt in the roll direction increased with increases of tilt in both the positive and the negative pitch direction (Fig. 13).

As shown in Fig. 14 and Fig. 15, the discrimination threshold for 0-degree tilt in the pitch direction stayed constant with increases of tilt in the positive roll direction (0 to +7º). Due to the symmetrical structure of the flat surface on the BioTac in the roll direction, similar discrimination thresholds are expected in the negative roll direction.

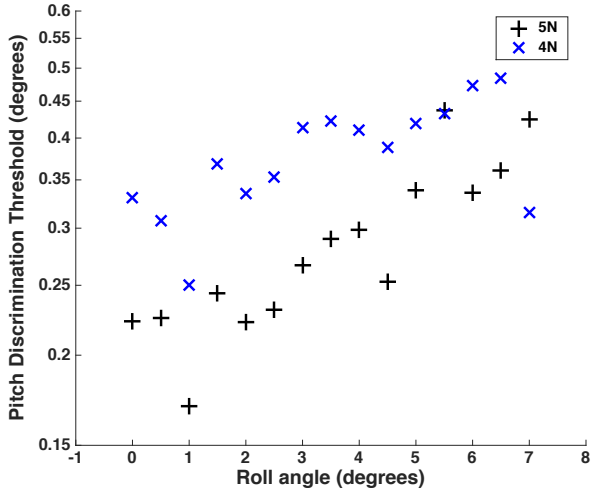

Figure 14. Effect of different roll angles on the discrimination thresholds (log scale) for 0-degree tilt along the pitch direction under only electronic noises.

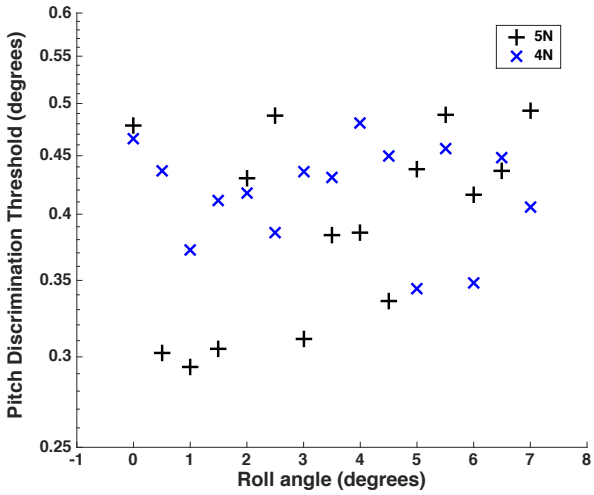

Figure 15. Effect of different roll angles on the discrimination thresholds (log scale) for 0-degree tilt along the pitch direction under both electronic noises and uncertainties in normal contact force.

D. *Utility of Various BioTac Electrodes for the Discrimination Thresholds for Tilts*

As the tilt between the sensorized flat portion of the BioTac and the surface of interest gets larger, it is possible that other sensorized surfaces of the BioTac might provide more information about incremental tilt angle. As shown in Fig. 16, the black plus sign ('+') compares the discrimination thresholds for 0-degree tilt in the roll direction based on electrodes 8 and 9 to the discrimination thresholds based on the voltage asymmetries between electrodes 2 and 12 on the half cylindrical part of the BioTac (red circles). Whereas the voltage asymmetries between electrodes 8 and 9 could detect tilts in roll when the pitch angle is in a wide range (-25 to +7º), the voltage asymmetries between electrodes 2 and 12 could only detect tilts in roll when the pitch angle is between -29º and -12º at 5N normal force level. Except at -24º, the discrimination thresholds using voltage asymmetries between electrodes 2 and 12 were larger than the discrimination thresholds using voltage asymmetries between electrodes 8 and 9.

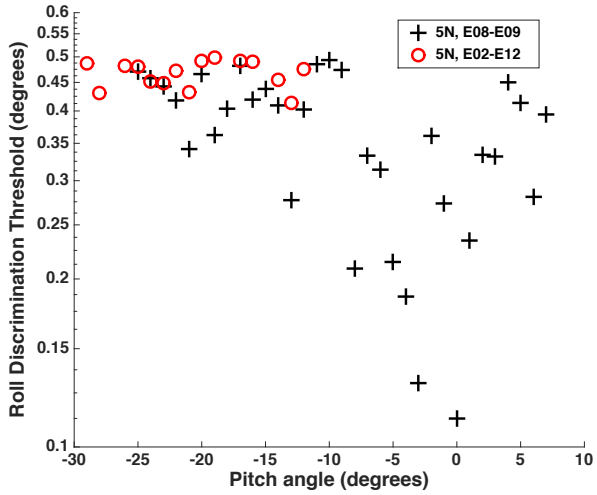

Figure 16. Comparison of tilt discrimination thresholds (log scale) for different electrode pairs.

V. Discussions and Conclusion

We have demonstrated the utility of a flat surface on a biomimetic tactile sensor, which mimics the most sensitive portion of the human distal phalanx (apical tuft), for detection of tilt of a contacting surface. The four impedance-sensing electrodes on the flat surface of the sensor could be used to detect as small as 0.11º of tilt in the roll direction and 0.19º in the pitch direction with respect to a flat, parallel object surface. Somewhat larger tilts could be detected over a wide range of tilt angles (±6.5º) in both roll and pitch directions. It could also detect tilt angles in the roll direction when tilt angle in the pitch direction was varied over a wide range (-27 to +7º), and it detected tilt angles in the pitch direction when tilt angle in the roll direction was varied from 0 to +7º.

Industrial robots often use custom rigid fixtures to hold specific tools in precise orientations with respect to the robotic linkage. There is increasing interest in general purpose robotic grippers that can handle a variety of tools and other objects similarly to human hands. Such grippers are likely to include some compliance to adjust for uncertainties in the size and shape of such objects, which in turn will result in some uncertainty of object orientation when subjected to mechanical loads. The BioTac provides a compliant gripping surface similar to human fingertips and the necessary tactile sensors to resolve small tilting movements between the object and the fingertips. The next step will be to integrate this tactile feature into a manipulation algorithm to achieve human-level dexterity during tool-use.

Because humans also have a flat surface on the end of each distal phalanx – the apical tuft – we hypothesize that humans could also benefit from using the flat surface when perceiving tilts. This could be tested by measuring the human discrimination threshold for tilt perception as a function of the location and orientation of the contact surface relative to the apical tuft.

REFERENCES

[1] R. S. Dahiya, G. Metta, M. Valle, and G. Sandini, "Tactile sensing—from humans to humanoids," *IEEE Transactions on Robotics,* vol. 26, pp. 1-20, 2010.

[2] Y. Chebotar, O. Kroemer, and J. Peters, "Learning robot tactile sensing for object manipulation," in *proc. IEEE/RSJ International Conference on Intelligent Robots and Systems*, 2014, pp. 3368-3375.

[3] H. Hoffmann, Z. Chen, D. Earl, D. Mitchell, B. Salemi, and J. Sinapov, "Adaptive robotic tool use under variable grasps," *Robotics and Autonomous Systems,* vol. 62, pp. 833-846, 2014.

[4] N. Wettels, L. M. Smith, V. J. Santos, and G. E. Loeb, "Deformable skin design to enhance response of a biomimetic tactile sensor," in *proc. 2nd IEEE RAS & EMBS International Conference on Biomedical Robotics and Biomechatronics*, 2008, pp. 132-137.

[5] Z. Su, J. A. Fishel, T. Yamamoto, and G. E. Loeb, "Use of tactile feedback to control exploratory movements to characterize object compliance," *Active Touch Sensing,* p. 51, 2014.

[6] Z. Su, Y. Li, and G. E. Loeb, "Estimation of Curvature Feature Using a Biomimetic Tactile Sensor," in *proc. American Society of Biomechanics*, 2011.

[7] N. Wettels and G. E. Loeb, "Haptic feature extraction from a biomimetic tactile sensor: force, contact location and curvature," in *proc. IEEE International Conference on Robotics and Biomimetics*, pp. 2471-2478.

[8] M. Shrewsbury and R. K. Johnson, "The fascia of the distal phalanx," *J Bone Joint Surg Am,* vol. 57, pp. 784-788, 1975.

[9] S. Almécija, S. Moyà-Solà, and D. M. Alba, "Early origin for human-like precision grasping: a comparative study of pollical distal phalanges in fossil hominins," *PLoS One,* vol. 5, p. e11727, 2010.

[10] J. R. Napier, "The prehensile movements of the human hand," *Bone & Joint Journal,* vol. 38, pp. 902-913, 1956.

[11] R. L. Susman, "Comparative and functional morphology of hominoid fingers," *American journal of physical anthropology,* vol. 50, pp. 215-236, 1979.

[12] M. M. Shrewsbury and R. K. Johnson, "Form, function, and evolution of the distal phalanx," *The Journal of hand surgery,* vol. 8, pp. 475-479, 1983.

[13] M. W. Marzke and M. S. Shackley, "Hominid hand use in the Pliocene and Pleistocene: evidence from experimental archaeology and comparative morphology," *Journal of Human Evolution,* vol. 15, pp. 439-460, 1986.

[14] R. L. Susman, "Hand of Paranthropus robustus from Member 1, Swartkrans: fossil evidence for tool behavior," *Science,* vol. 240, pp. 781-784, 1988.

[15] M. W. Marzke and R. F. Marzke, "Evolution of the human hand: approaches to acquiring, analysing and interpreting the anatomical evidence," *Journal of anatomy,* vol. 197, pp. 121-140, 2000.

[16] E. S. Mittra, H. F. Smith, P. Lemelin, and W. L. Jungers, "Comparative morphometrics of the primate apical tuft," *American journal of physical anthropology,* vol. 134, pp. 449-459, 2007.

[17] M. W. Marzke, "Precision grips, hand morphology, and tools," *American Journal of Physical Anthropology,* vol. 102, pp. 91-110, 1997.

[18] E. R. Serina, C. D. Mote, and D. Rempel, "Force response of the fingertip pulp to repeated compression—effects of loading rate, loading angle and anthropometry," *Journal of biomechanics,* vol. 30, pp. 1035-1040, 1997.

[19] G. Westling and R. S. Johansson, "Responses in glabrous skin mechanoreceptors during precision grip in humans," *Experimental Brain Research,* vol. 66, pp. 128-140, 1987.

[20] A. B. Vallbo and R. S. Johansson, "The tactile sensory innervation of the glabrous skin of the human hand," *Active touch,* vol. 2954, pp. 29-54, 1978.

[21] R. S. Johansson and Å. B. Vallbo, "Detection of tactile stimuli. Thresholds of afferent units related to psychophysical thresholds in the human hand," *The Journal of physiology,* vol. 297, p. 405, 1979.

[22] H. Ogawa, "The Merkel cell as a possible mechanoreceptor cell," *Progress in neurobiology,* vol. 49, pp. 317-334, 1996.

[23] J. R. Phillips and K. O. Johnson, "Tactile spatial resolution. II. Neural representation of bars, edges, and gratings in monkey primary afferents," *Journal of neurophysiology,* vol. 46, pp. 1192-1203, 1981.

[24] A. W. Goodwin, A. S. Browning, and H. E. Wheat, "Representation of curved surfaces in responses of mechanoreceptive afferent fibers innervating the monkey's fingerpad," *The Journal of neuroscience,* vol. 15, pp. 798-810, 1995.

[25] E. R. Serina, E. Mockensturm, C. D. Mote, and D. Rempel, "A structural model of the forced compression of the fingertip pulp," *Journal of biomechanics,* vol. 31, pp. 639-646, 1998.

[26] J. Voisin, G. Benoit, and C. E. Chapman, "Haptic discrimination of object shape in humans: two-dimensional angle discrimination," *Experimental brain research,* vol. 145, pp. 239-250, 2002.

[27] I. Toderita, S. Bourgeon, J. I. A. Voisin, and C. E. Chapman, "Haptic two-dimensional angle categorization and discrimination," *Experimental brain research,* vol. 232, pp. 369-383, 2014.

[28] M. W. A. Wijntjes, A. Sato, V. Hayward, and A. M. L. Kappers, "Local surface orientation dominates haptic curvature discrimination," *IEEE Transactions on Haptics,* vol. 2, pp. 94-102, 2009.

[29] G. De Maria, C. Natale, and S. Pirozzi, "Tactile data modeling and interpretation for stable grasping and manipulation," *Robotics and Autonomous Systems,* vol. 61, pp. 1008-1020, 2013.

[30] G. De Maria, C. Natale, and S. Pirozzi, "Force/tactile sensor for robotic applications," *Sensors and Actuators A: Physical,* vol. 175, pp. 60-72, 2012.